

Periplasmic Expression, Purification, and Characterization of an Anti-epidermal Growth Factor Receptor Antibody Fragment in *Escherichia coli*

Won-Jae Chi, Hyerim Kim, Heejung Yoo, Young Pil Kim, and Soon-Kwang Hong

Received: 23 December 2015 / Revised: 11 February 2016 / Accepted: 22 February 2016
© The Korean Society for Biotechnology and Bioengineering and Springer 2016

Abstract New structural designs of antibody fragments have considerable biotechnological and therapeutic potential. In this study, we describe the construction and functional expression of a cetuximab-based antibody fragment (scFv-C_H3, minibody) that exhibits activity against human colon cancer. Heterologous expression in *Escherichia coli* (*E. coli*) was improved by optimizing the host cells, signal peptides, induction conditions, and culture media. The recombinant minibody was expressed successfully in the periplasm of *E. coli* BL21(DE3) and purified by immobilized metal affinity chromatography using a Ni²⁺-NTA resin. The purified minibody showed high binding affinity to cell-surface epidermal growth factor receptor (EGFR) and exhibited inhibition of EGFR-mediated signal transduction in the human colon cancer cell line HT29 in a similar way by the cetuximab. The minibody also showed significant level of anti-cancer ability in the HT29 colorectal cancer xenograft model, which was lower than that by the cetuximab.

Keywords: minibody, anti-EGFR antibody, colon cancer, anti-cancer activity

1. Introduction

Epidermal growth factor (EGF) regulates cell growth, proliferation, and differentiation by interacting with EGF-receptor (EGFR) on the cell surface. EGFR is a member of the ErbB family of transmembrane receptor tyrosine kinases. It is highly expressed in various epithelial tumors and has been regarded as a target in the development of anti-cancer therapeutic reagents, including therapeutic antibodies. Interaction between EGF and EGFR stimulates mitogenic signal transduction *via* the activation of intrinsic protein tyrosine kinase activity and internalization of EGFR.

Cetuximab (Erbix[®]; Eli Lilly and Company, New York, USA; Bristol-Myers Squibb Company, Princeton, USA) is a human-mouse chimeric monoclonal whole immunoglobulin G1 (IgG1) antibody that specifically binds to EGFR. It is currently approved by the US Food and Drug Administration for the treatment of metastatic colorectal carcinomas (mCRC). Cetuximab binds to the extracellular ligand-binding domain of EGFR with higher binding affinity than does EGF. Its binding leads to the inhibition of EGFR-mediated signal transduction, inhibiting tumorigenesis and tumor growth [1]. It also induces the modulation of pro- and anti-apoptotic regulators in a variety of tumor cell lines [2].

Intact IgG antibodies have several limitations as anti-cancer therapeutic agents, including poor penetration into tumor tissues and high cost of production, because of their size and the requirement for a mammalian expression system, respectively. Several techniques have been developed to

Won-Jae Chi
Biological and Genetic Resources Assessment Division, National Institute of Biological Resources, Incheon 404-170, Korea

Hyerim Kim, Heejung Yoo, Young Pil Kim^{**}
Department of Bio-Engineering, Life Science RD Center, Sinil Pharmaceutical Co., Seongnam 462-815, Korea
Tel: +82-31-748-9117; Fax: +82-31-723-0807
E-mail: kyp2943@gmail.com

Soon-Kwang Hong^{**}
Division of Biological Science and Bioinformatics, Myongji University, Yongin 449-728, Korea
Tel: +82-31-330-6198; Fax: +82-31-335-8249
E-mail: skhong@mju.ac.kr

[†]These authors contributed equally to this work.

overcome these limitations. For example, recombinant antibody fragments—such as variable fragments (Fv), single-chain Fvs (scFv), Fabs, and minibodies (scFv-C_H3)—can contribute to low immunogenicity, high penetration, and low production costs [3]. In addition, the *E. coli* expression system for the production of antibodies has several advantages, including high expression level, rapid growth rate, low cost of cultivation, simple purification, non-glycosylation, and low risk of viral DNA contamination.

Recently, we reported production of an EGFR-specific minibody derived from the intact IgG1 antibody cetuximab in an engineered prokaryote, *Escherichia coli*, by modifying the length of peptide linker joining the variable heavy (V_H) and light (V_L) region. In addition, we proved that MI061 minibody with an 18-residue peptide linker had highly significant anti-tumor effect probably by inhibiting ERK pathway in the human epidermoid carcinoma cell line A431 and A431 xenograft mice [4]. In this study, production of an EGFR-specific minibody in *E. coli* was optimized by improving the expression conditions including secretory signal sequences, *E. coli* host cell strains, culture media, and induction conditions. The recombinant minibody was purified, and its anti-cancer EGFR-targeting ability was also confirmed in the human colon cancer cell line HT29 and HT29 xenograft model.

2. Materials and Methods

2.1. Bacterial strains and plasmid

E. coli DH5 α F⁺ was used for subcloning. The strains, *E. coli* BL21(DE3), *E. coli* BL21(DE3) pLysS, and *E. coli* C43(DE3) and the pET26b(+) vector were used for expression.

2.2. Media and culture conditions

E. coli was maintained in Luria-Bertani (LB) medium (Difco, BD, USA) at 37°C under agitation. The *E. coli* transformants were stored in 20% glycerol stock at -80°C. The fine chemicals were purchased from Sigma-Aldrich Corporation (USA).

2.3. Construction of expression plasmids with different signal sequences

To construct the minibody (scFv-C_H3), a DNA fragment encoding the V_H and V_L domains was synthesized based on the amino acid sequence of the cetuximab Fab. The linker consisted of 18 amino acids (GSTSGSGKPGSGEGSTKG) between the V_H and V_L domains and was modified and synthesized based on the amino acid sequences of the m218 Whitlow linker [5]. The Hinge-C_H3 domain was synthesized based on the amino acid sequences of human IgG1, with the exception of a modified amino acid sequence (EPKSPKSADKHTHTAP) that was used for the hinge region. The domain order of variable chains, the V_L-C_L and V_H-C_H1 domains, the linker length and sequence, and the sequence of the hinge region were determined according to the findings of our previous study [4].

Expression plasmid MI061 containing the V_H-Linker-V_L domain and the Hinge-C_H3 domain was constructed as described in the previous report [4]. The codons were optimized for *E. coli* expression. MI061 contains a scFv in the order of the V_H-Linker-V_L-Hinge-C_H3 with pelB (pectate lyase B) signal sequence (MKYLLPTAAAGLLLLAAQ PAMA) for secretion [6]. The *pelB* signal sequence of MI061 was replaced with *ompA* (outer-membrane A) signal sequence (MKKTAIAIAVALAGFATVAQA), yielding MI046 [7]. The signal sequence of MI061 was also replaced with a modified eukaryotic signal peptide, c26B (MRFSTTLATAATALFFFTASQVSA), giving MI125 [8]. The primers used are listed in Table 1.

2.4. Determination of expression conditions

2.4.1. Signal sequence

The plasmids MI046, MI061, and MI125 were transformed and expressed in *E. coli* BL21(DE3). The transformants were cultured in 100 mL of LB broth (50 μ g/mL kanamycin) at 37°C until an OD_{600 nm} of 0.5 was reached. Protein expression was induced by the addition of 0.1 mM isopropyl β -D-1-thiogalactopyranoside (IPTG), after which the transformants were cultured at 20°C for 18 h. The culture broth was collected at regular intervals. Crude extracts were

Table 1. Oligonucleotides used in this study

Name	Sequence (5' to 3')*	Characteristics
MI046-F1	<u>GGATCC</u> ATGAAAAAGACAGCTATCGCAATTGCAGTGGCCCTGGCTGGTTTC GCTACCGTAGCGCAAGCTACAAGTCCAAGTCAAACAATCG	Restriction enzyme site: <i>Bam</i> HI Signal peptide sequence: <i>OmpA</i>
MI046-R1	CTGTCCCTGTCTCCGGGTAA <u>ACTCGAGGCG</u>	Restriction enzyme site: <i>Xho</i> I
MI125-F1	<u>GGATCC</u> ATGCGTTTTAGTACGACACTGGCGACGGCCGCAACGGCCCTCTT CTTACGGCGAGTCAGGTAAGCGCGACAAGTCCAAGTCAAACAATCG	Restriction enzyme site: <i>Bam</i> HI Signal peptide sequence: C26B
MI125-R1	CTGTCCCTGTCTCCGGGTAA <u>ACTCGAGGCG</u>	Restriction enzyme site: <i>Xho</i> I

*Underlines and italic letters indicate restriction enzyme sites and signal sequences, respectively.

prepared from the collected samples by sonication and used for western blot analysis.

2.4.2. Host for expression

MI061 was transformed into *E. coli* BL21(DE3), *E. coli* BL21 codon plus, *E. coli*(DE3) pLysS, and *E. coli* Rosetta-gami(DE3). The transformants were cultured and protein expression was induced and analyzed by the same protocols as explained above.

2.4.3. Induction conditions

To determine the proper concentration of inducer, protein expression was induced by IPTG at various concentrations (0.01, 0.02, 0.03, 0.04, 0.05, 0.1, 0.2, 0.4, 0.6, 0.8, and 1.0 mM) at an OD_{600 nm} of 0.5 in MI061/*E. coli* BL21(DE3). To determine the induction point, the transformants were divided into three groups, each cultured to an OD_{600 nm} of 0.5, 1.0, or 1.3, and protein expression was induced by the addition of IPTG at a final concentration of 0.05 mM. The transformants were then further cultured at 20°C for 12 h. Protein expression levels were analyzed by western blot analysis.

2.4.4. Culture media

MI061/*E. coli* BL21(DE3) was cultured in 100 mL LB (pH 8.0), LB trace element, LB5X, LB5X glucose, LB5X glycerol, Super Broth (SB, Difco, BD, USA), 2X YT (Difco, BD, USA), M9 (Difco, BD, USA), YM9 glucose, YM9 glycerol, SOC, SOB, or Terrific Broth (TB, Difco, BD, USA) in a 500 mL baffled flask. The medium compositions used are listed in Table 2. Protein expression was induced by the addition of 0.05 mM IPTG at an OD_{600 nm} of 1.3, and the transformants were then further cultured at 20°C for 12 h. Crude extracts prepared from the cells were used for western blot analysis.

2.5. Purification of the minibody

E. coli strains harboring different plasmids were cultured in 10 mL LB broth in a 100 mL baffled flask at 30°C for 12 h under vigorous shaking. For each, 1% of seed culture was inoculated in 1 L LB broth in a 3 L baffled flask and further cultured at 37°C until an OD_{600 nm} of 1.0 was reached. Protein expression was induced by the addition of IPTG (0.05 mM), and the cells were further cultured for 12 h. The cells were harvested by centrifugation at 8,000 g for 10 min. To extract soluble recombinant proteins from the periplasm [9], the harvested cells were resuspended in 100 mL of spheroplast solution (50 mM Tris-HCl (pH 8.0), 20% (w/v) sucrose and 1 mM EDTA), left for 20 min on ice and harvested by centrifugation at 4°C and 6,200 g for 10 min. The supernatant (periplasmic enriched fraction) was cleared by centrifugation at 4°C and 30,000 g for 30 min,

Table 2. Composition of culture media used in this study

No.	Media	Composition (g/L)
1	LB	Tryptone 10.0 Yeast extract 5.0 NaCl 5.0
2	LB	LB (pH was adjusted to 8.0 before sterilization.) (pH 8.0)
3	LB trace element	LB base Trace element solution 2 mL
4	LB5X	Tryptone 50.0 Yeast extract 25.0 NaCl 25.0
5	LB5X glucose	LB5X base Glucose 4.0
6	LB5X glycerol	LB5X base Glycerol 4 mL
7	SB (Difco)	Casein enzymatic hydrolysate 32.0 Yeast extract 20.0 NaCl 5.0
8	2XYT (Difco)	Bacto tryptone 16.0 Yeast extract 10.0 NaCl 5.0
9	M9 (Difco)	a. Mix the M9 salts (at 1X) by combining, per liter: Na ₂ HPO ₄ 6.0 KH ₂ PO ₄ 3.0 NaCl 5.0 NH ₄ Cl 1.0 Water up to 800 mL b. Filter sterilize or autoclave. c. Add the following sterile components (per liter): 100 mM CaCl ₂ 1 mL 1 M MgSO ₄ 1 mL Glycerol 0.3% final Sterile Water up to 1 L final
10	YM9 glucose	M9 base Yeast extract 10.0 Glucose 4
11	YM9 glycerol	M9 base Yeast extract 10.0 Glycerol 4 mL
12	SOC	Tryptone 20.0 Yeast extract 5.0 NaCl 10 mM KCl 5 mM MgCl ₂ 10 mM Glucose 20 mM
13	SOB	Tryptone 20.0 Yeast extract 5.0 NaCl 10 mM KCl 2.5 mM MgCl ₂ 10 mM
14	TB (Difco)	Pancreatic digest of casein 12.0 K ₂ HPO ₄ 9.4 KH ₂ PO ₄ 2.2 Glycerol 4 mL

and dialyzed against PBS (phosphate-buffered saline). The extract was passed through a Ni²⁺-NTA column (GE Healthcare, Sweden) pre-equilibrated with PBS. After subsequent washing with 10 bed volumes of PBS, recombinant

proteins with the carboxyl-terminal His-tag of the C_{H3} domain were eluted by stepwise gradient elution using 20 ~ 400 mM imidazole in 1X PBS. The eluate was analyzed on 0.1% SDS-10% PAGE. Ligand-binding activity of the fractions was measured by an enzyme-linked immunosorbent assay (ELISA).

2.6. Western blot analysis

Protein samples were loaded onto an SDS-PAGE gel and transferred to a polyvinylidene fluoride (PVDF) membrane, then immunoblotted with the primary anti-C_{H3} domain antibody A567H and a secondary HRP-conjugated anti-mouse IgG antibody (Thermo Fisher Scientific Inc., USA).

2.7. Enzyme-linked immunosorbent assay (ELISA)

To determine the ligand-binding activity of each protein sample, a 96-well immunoplate was coated with 0.1 µg of sEGFR in 200 mM Na₂CO₃ (pH 9.6) and incubated overnight at 4°C. The plate was washed and blocked with bovine serum albumin (BSA) solution. The protein sample was added and incubated for 1 h at room temperature, then washed with PBS containing Tween 20 (PBS-T). The primary anti-C_{H3} domain antibody A567H was added, and the sample was incubated for 1 h at room temperature and washed with PBS-T, followed by incubation with the secondary HRP-conjugated anti-mouse IgG antibody. Color development was performed using the chromogenic HRP substrate TMB (Sigma-Aldrich Corporation, USA) and terminated with 1 M H₂SO₄. The chromogenic signal was detected at 450 nm.

2.8. Flow cytometric analysis

The ligand-binding ability of MI061 was measured by flow cytometry (fluorescence activated cell sorting) analysis using the human colon cancer cell line HT29, which exhibits a high level of EGFR expression. HT29 was purchased from the American Type Culture Collection. HT29 cells at a final concentration of 1×10^5 cells/well were treated either with an anti-EGFR mAb (cetuximab) or with MI061, each at a concentration of 2 µg/mL for 30 min at 4°C and washed with 1% BSA in PBS. A FITC-labeled goat anti-human Fc mAb (Sigma-Aldrich Corporation, USA) was added to reach a final concentration of 4 µg/mL, and the cells were incubated for 30 min. Signals were detected by an Accuri C6 flow cytometer (BD Biosciences, USA).

For the competition assay, the HT29 cells were incubated with a FITC-labeled EGF ligand (Molecular Probes, Leiden, The Netherlands) at a final concentration of 6 nM and MI061 at a final concentration of 2 µg/mL for 30 min at 4°C. After subsequent washing, the cells were analyzed by an Accuri C6 flow cytometer to determine the relative amounts of bound FITC-labeled EGF.

2.9. Apoptosis analysis using annexin V

Cells at a final concentration of 5×10^4 cells/well were seeded in a 6-well plate containing RPMI1640 and 10% FBS and incubated for 24 h at 37°C. Following this, the cells were starved under the conditions of 0.1% FBS and RPMI1640 for 24 h at 37°C. After treatment with cetuximab and MI061 at a final concentration of 2 µg/mL each for 48 h, the media were collected and washed with 1X PBS and 1X binding buffer. Cell density in the 1X binding buffer was 1×10^6 cells/mL. Then, 5 µL of Annexin V-FITC was added to 195 µL of sample, mixed, and incubated for 10 min at room temperature in the dark. After washing with 1X binding buffer twice, 190 µL of fresh 1X binding buffer and 5 µL of propidium iodide were added to the cell suspension. Signals were detected by an Accuri C6 flow cytometer. To detect apoptosis, the Annexin V-FITC Apoptosis Detection Kit (eBioscience, USA) was used according to the protocol supplied by the manufacturer.

2.10. Xenograft tumor assay

Human colon cancer xenografts were established by injecting 5×10^6 HT29 tumor cells subcutaneously (s.c.) into the left flank of 6- to 7-week-old male nude athymic (nu/nu) mice. This mouse strain is often used in cancer research because the mice are genetically engineered to be T-cell deficient, which allows for the routine and efficient transplantation and propagation of established human tumor cell lines. Tumor volume was calculated once every 3 days using a digital caliper and the following formula: Volume (mm³) = length (mm) × width (mm) × height (mm). Once tumor volume reached 100 mm³ in each group, the mice were randomized into three subgroups of six animals each. Then, 100 µL of sterilized PBS (q3d) as the control, cetuximab (0.25 mg/mouse, q3d), or MI061 (0.25 mg/mouse, qd) was intraperitoneal (i.p.) administered to each mouse. All animal experiments in this study were performed in accordance with the guidelines of the Institutional Animal Care and Use Committee (IACUC) of Konkuk University (<http://www.mfds.go.kr/index.do>). The study conducted herein was approved by the Konkuk University IACUC (Approval No.: KU14024). The mice were purchased from Nara Biotech (Seoul, Korea).

2.11. Immunohistochemistry analysis

After euthanization by CO₂ asphyxiation, the tumors were excised from mice, fixed with 10% formalin, and embedded in paraffin. The embedded tissues were sectioned with a microtome into slices 4 ~ 5 µm thick. The paraffin was then completely removed with xylene for analysis of antigen-antibody interactions. Formalin-fixed and paraffin-embedded tissue sections on slides were covered with 3% H₂O₂ for 10 min at room temperature to block endogenous

peroxidase. For detection of total EGFR, the slides were incubated with a primary anti-EGFR antibody (Cell Signaling Technology, USA) for 18 h at 4°C. The slides were then washed with TBS (Tris-buffered saline) and incubated with a secondary antibody (Dako, Japan) for 30 min at room temperature. Total EGFR in each tissue section was visualized by treating with a DAB (3, 3'-diaminobenzidine) substrate chromogen solution. For analysis of phosphorylated EGFR (pEGFR), pre-processing steps were performed as described above. To prevent nonspecific interactions, the tissue sections were blocked with protein block serum-free solution for 10 min at room temperature. After incubation with a primary antibody, pEGFR (Tyr845) for 18 h at 4°C, the slides were reacted with a secondary antibody for 15 min at room temperature and 10 min incubation with tyramide for signal amplification. Finally, the slides were counterstained with hematoxylin and dehydrated before mounting.

2.12. Pharmacokinetics analysis

To perform pharmacokinetics (PK) analysis, 100 µL blood samples were collected from mice injected with MI061 (i.p., 0.3 mg/mouse) at 1, 3, 6, 24, and 48 h after the initial injection. After centrifugation at 15,000 g for 5 min, serum was transferred to a new tube and stored at -80°C. The pharmacokinetic analysis was performed using non-compartmental methods according to the BA cal2007 guidelines [10] set out by the Korea Food and Drug Administration (now the Ministry of Food and Drug Safety).

3. Results

3.1. Construction and expression of anti-EGFR antibody fragment

The antibody fragment minibody (scFv-C_H3) based on cetuximab was cloned into pET26b—with the PelB leader sequence at the amino terminal region and 6 histidine residues at the carboxyl terminal region (in MI061) and expressed in *E. coli* BL21(DE3). In some cells, the PelB leader sequence was replaced by OmpA (in MI046) and c26B (in MI125) to allow for comparison of secretory production of the recombinant protein (Fig. 1). Protein production of the three different signal peptides was compared by western blot analysis (Fig. 2A). The scFv-C_H3-His chimeric protein is composed of 360 amino acids and its expected molecular weight (MW) is 43 kDa. The expression of MI061 (a 45 kDa protein corresponding to the MW deduced from the amino acid sequence of MI061 with his-tag) rapidly increased after induction and was maintained during 15 h of cultivation. Although protein production by MI046 also rapidly increased after induction,

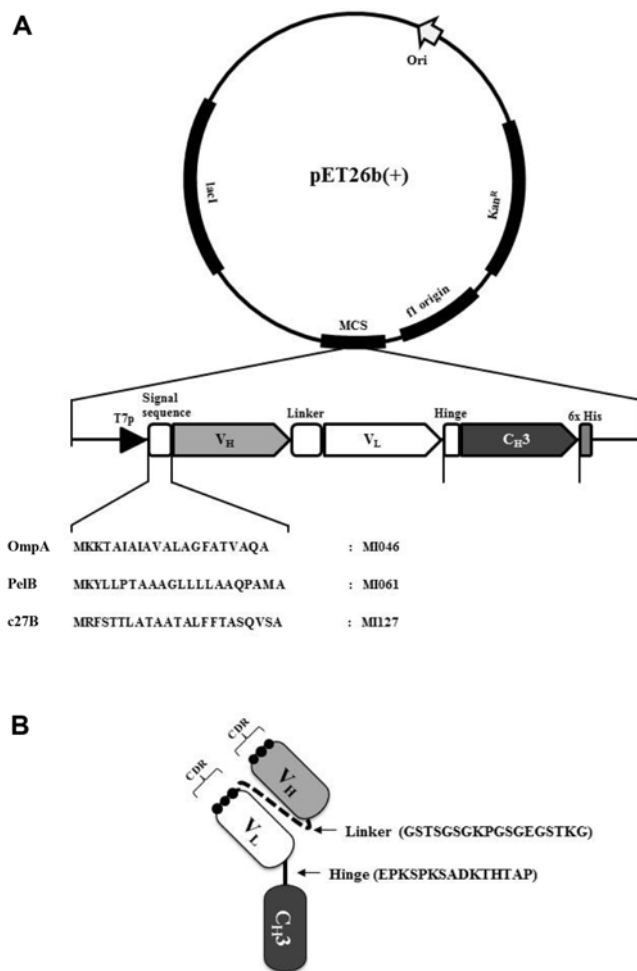


Fig. 1. Schematic presentation of minibody expression constructs (A) and predicted structure of the minibody (B). (A) Construction of expression vectors for the three different signal peptide-fused minibodies. The amino terminal region of the V_H domain was linked with the three signal peptides: PelB (21 aa), OmpA (22 aa), and C26B (23 aa). The carboxyl terminal region of C_H3 domain was followed by six histidine residues. (B) Predicted structure of monovalent minibody. The purified MI061 was expected to assemble into a divalent molecule with a molecular weight of 90 kDa by hydrophobic interactions between the C_H3 domains. Linker and hinge regions are represented by the dotted line and bold line, respectively. CDR regions in the V_H and V_L domains are represented by three filled circles.

it gradually decreased after 6 h of cultivation. In MI125, however, the yield gradually increased until 5 h of cultivation, whereupon it was maintained, and then decreased after 15 h of cultivation. Among the tested signal peptides, the PelB leader sequence gave the highest final protein yield after 12 h of cultivation.

3.2. Optimization of expression conditions

The MI061 construct was transformed and expressed in various *E. coli* strains, and protein expression was compared

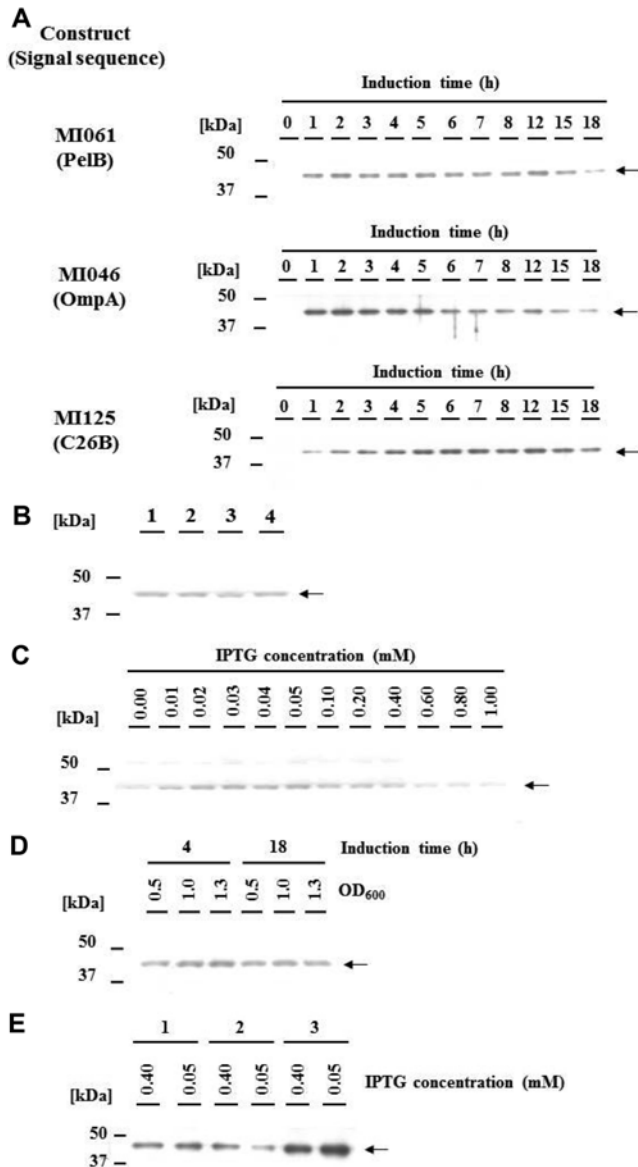


Fig. 2. Optimization of minibody expression in *E. coli*. (A) Comparison of signal sequences. At different times after induction, cells were harvested, and minibody expression was measured by western blot using the primary anti- C_{H3} domain antibody A567H. PelB signal sequence (upper panel). OmpA signal sequence (middle panel). C26B signal sequence (lower panel). (B) Comparison of the expression hosts. Expression levels of minibody MI061 in different hosts were detected by western blot analysis. 1, *E. coli* BL21(DE3); 2, *E. coli* BL21 codon plus; 3, *E. coli* BL21(DE3) pLysS; 4, *E. coli* Rosetta-gami(DE3). (C) Determination of optimal IPTG concentration. Minibody expression was induced at an $OD_{600\text{ nm}}$ of 0.5 with various concentrations of IPTG, and minibody MI061 expression levels were detected by western blot analysis. (D) Determination of optimal induction point. MI061 expression was induced at three different $OD_{600\text{ nm}}$ values with 0.05 mM IPTG. (E) Comparison of culture media. Expression of MI061 was compared in various media:—1, LB; 2, LB trace element; 3, YM9 glucose—at different IPTG concentrations; 0.05 mM and 0.4 mM. Expression levels were measured by western blot analysis. Arrows indicate recombinant protein and molecular weights are indicated at the left of the gel (A–E).

by western blot analysis. No significant differences in expression level were observed among the different hosts (Fig. 2B). However, MI061/*E. coli* BL21(DE3) had the highest final yield as indicated by its cell mass under culture conditions being the highest among that of all hosts.

The productivity of the soluble recombinant protein gradually increased as IPTG concentrations increased from 0.01 to 0.05 mM, but decreased at higher inducer concentrations; 0.1 ~ 1.0 mM (Fig. 2C). To determine the optimal induction point, IPTG was added at various optical densities ($OD_{600\text{ nm}}$ of 0.5, 1.0, and 1.3). The highest protein expression level was observed in cells induced at an $OD_{600\text{ nm}}$ of 1.3 after 4 h cultivation, but there was no significant difference in expression levels among the 12 h cultivation samples (Fig. 2D).

When MI061/*E. coli* BL21(DE3) was cultured in various media, protein productivity was highest in the YM9 glucose medium at 12 h after induction (Fig. 2E, Supplementary data S1).

3.3. Purification of the Minibody

The total expression level of MI061 in *E. coli* BL21(DE3) under the optimized condition was investigated on SDS-PAGE. Although the production conditions of the recombinant protein were improved, almost 90% of the expressed proteins were found to be inactive inclusion bodies (Supplementary data S2).

MI061 was purified from the periplasm of *E. coli* by nickel-affinity column chromatography. The purity and identity of the purified protein were confirmed by SDS-PAGE and western blot analysis, respectively (Fig. 3A). The MW and purity of the purified MI061 was estimated to be 45 kDa and about 95%, respectively (Fig. 3A). However, purified MI061 was estimated to be 90 kDa by size exclusion chromatography using a BioSep-SEC-s2000 column (300 × 7.8 mm, Phenomenex, USA), which corresponds to the MW of the dimeric form. Although MI061 has a hinge region without free intermolecular cysteine residues, it was expected to be assembled into dimeric form through hydrophobic interactions between the C_{H3} domains [4].

3.4. The EGFR signal pathway is inhibited by MI061

When the immunoreactivity of purified MI061 was determined by ELISA, it exhibited strong activity against the sEGFR antigen. When total expression levels of EGFR were estimated in the colon carcinoma cell lines A431, HCT116, and HT29 by FACS analysis, all cell lines exhibited a high level of EGFR expression (data not shown). Among them, HT29 was selected for further study because it is well-known as an EGFR-positive cell line and satisfies the criteria for cetuximab therapy [11]. The ligand-

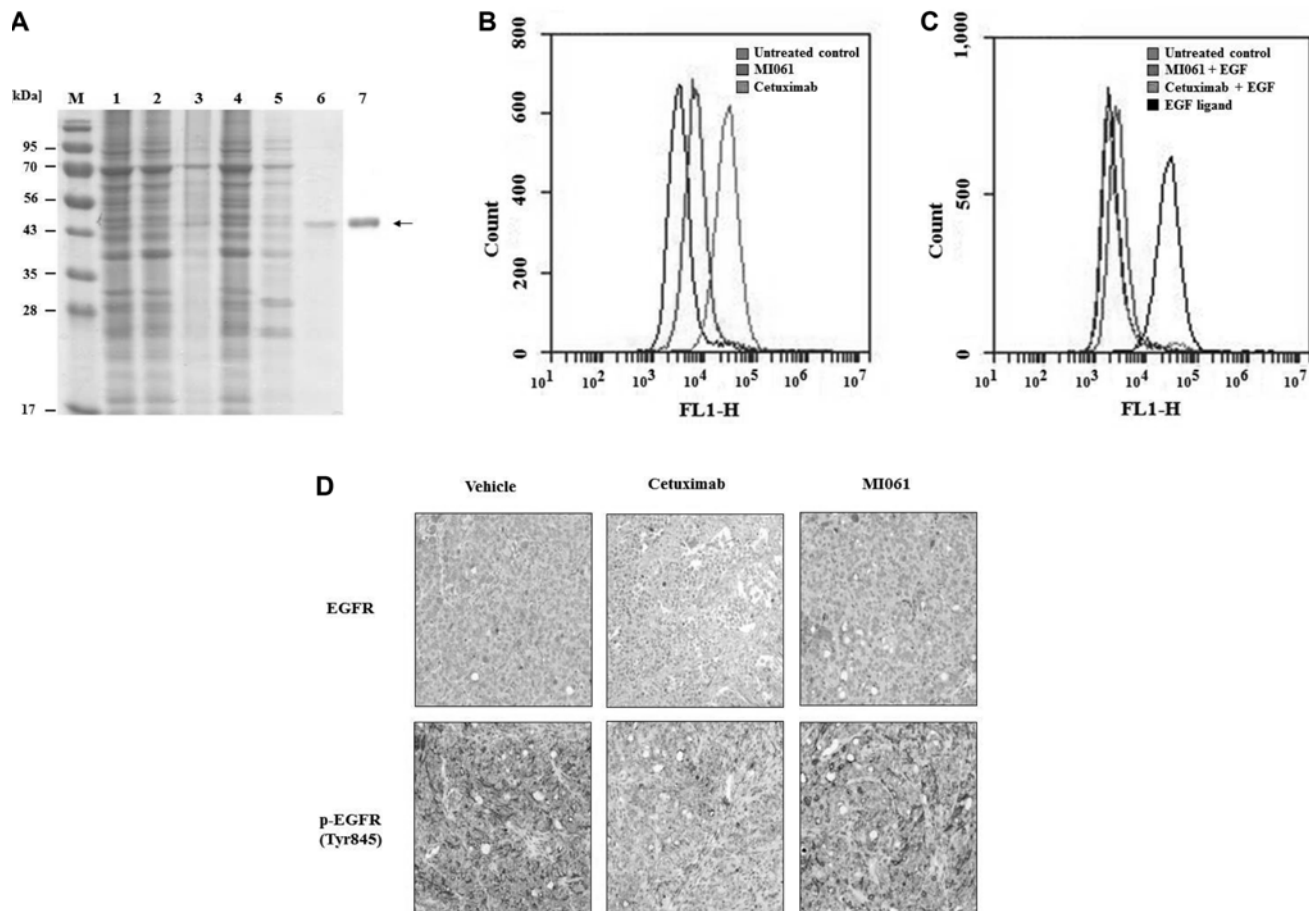


Fig. 3. Purification of MI061. (A) SDS-PAGE analysis of purified MI061. 1, soluble proteins; 2, flow through; 3, washing with 1X PBS; 4, washing with 1X PBS containing 20 mM imidazole; 5, washing with 1X PBS containing 50 mM imidazole; 6, elution with 400 mM imidazole; 7, western blot analysis of elution sample. (B) EGFR binding assay of MI061. MI061 was incubated with EGFR-overexpressed HT29 cells, and binding activities were analyzed by FL1-H intensity using flow cytometry (FACS) analysis. Cetuximab was used as a positive control. (C) EGFR competition assay of MI061. HT29 cells were co-incubated with FITC-labeled EGF ligand and MI061. Cetuximab was used as a positive control. (D) Phosphorylation assay of EGFR. The inhibitory effect of MI061 on phosphorylation of EGFR in HT29 cells was analyzed by IHC staining using a p-EGFR (Tyr845) primary antibody. Cetuximab was used as a positive control.

binding ability between MI061 and HT29 was measured by FACS analysis. Although the fluorescence signal of the MI061-treated sample was weaker than that of cetuximab-treated sample (control), the MI061-treated sample exhibited a shifted signal greater than that of the untreated negative control (Fig. 3B). A competition binding assay of purified MI061 was carried out using a FITC-labeled EGF ligand, which is an activator of the EGFR pathway that regulates key processes in cell biology, including proliferation, survival, and differentiation. Treatment with MI061 partially inhibited the interaction between EGF and EGFR, whereas treatment with cetuximab as a positive control entirely inhibited the interaction (Fig. 3C).

Expression levels of total EGFR and phospho-EGFR (pEGFR) were analyzed by immunohistochemistry (IHC) with HRP-DAB on the xenograft tumor sections. As

shown in Fig. 3D, levels of both EGFR and pEGFR were slightly lower in the MI061-treated group than in the vehicle group (a negative control). Notably, decreased EGFR and pEGFR expression was found in the cetuximab-treated group. These results suggest that MI061 inhibited the pEGFR-mediated signal pathway by competitively binding with EGF in the human colon cancer cell HT29 in a similar way as reported in the human epidermoid carcinoma cell A431 [4].

3.5. Tumor growth in human colon cancer xenografts is inhibited by MI061

Pharmacokinetics (PK) parameters in the HT29 xenograft were estimated to characterize the PK of the recombinant cetuximab-based minibody, MI061. The measured C_{max} , T_{max} , area under the curve (AUC), and $t_{1/2}$ were 10.2 mg/L,

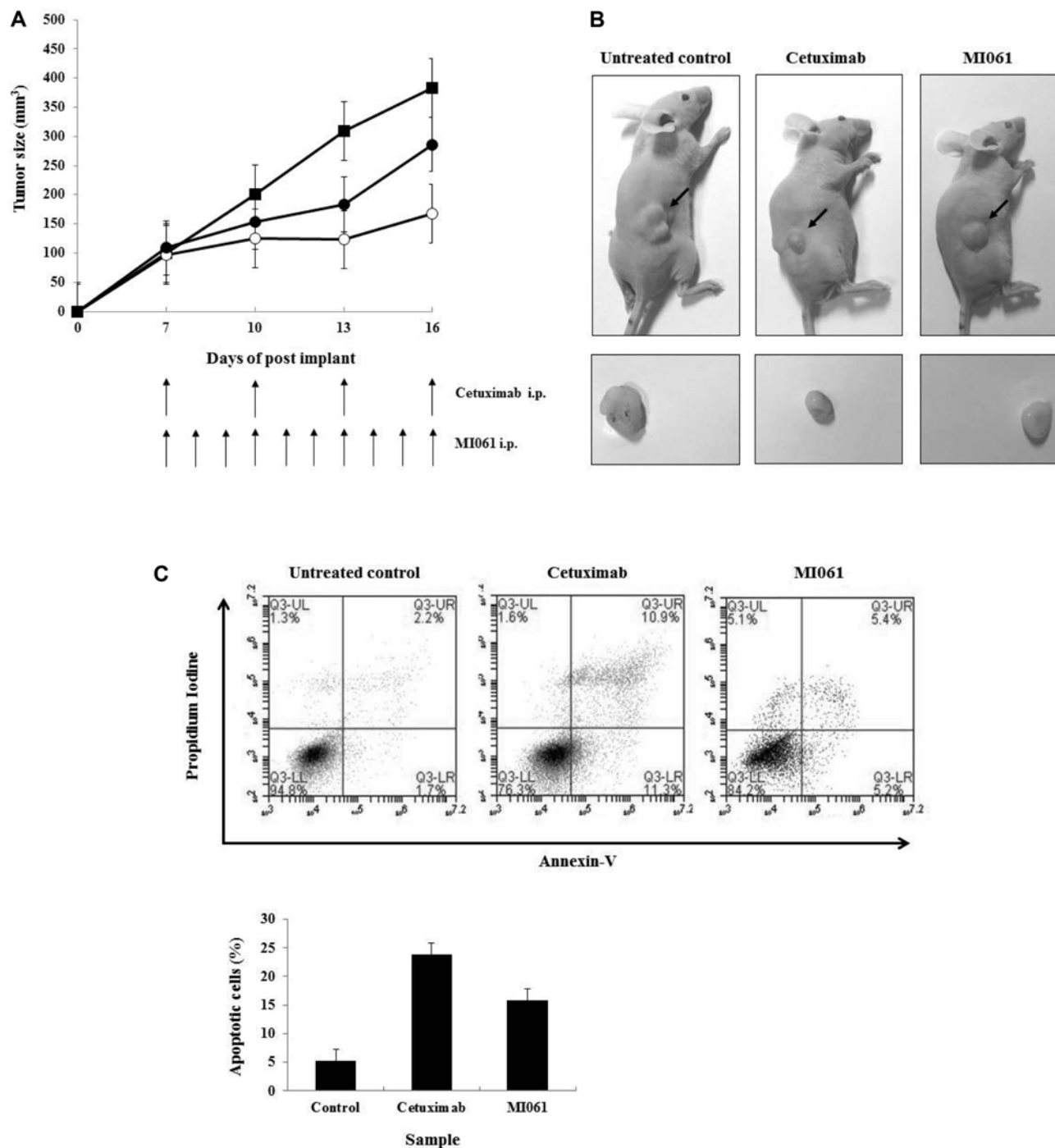


Fig. 4. Antitumor effect of MI061 in HT29 xenograft mouse model. (A) Antitumor activity of MI061. MI061 was administered intraperitoneally every day whereas cetuximab was administered every 3 days. Treatment was continued for 16 days and mice were sacrificed at day 16. Tumor growth was monitored by measuring tumor volume and is expressed as the mean value for each treatment group ($n = 6$). ■, vehicle control; ●, MI061; ○, cetuximab. (B) Representative tumor formation in nude mice bearing HT29 cells. Arrows indicate tumor masses established on the left flank of athymic mice (upper panel). Photographs of tumor masses excised from HT29 xenograft mice (lower panel). (C) Apoptotic analysis by FACS. Apoptotic signaling by MI061 in HT29 cells was analyzed by an Accuri C6 flow cytometer (upper panel). Column diagrams showing percentages of apoptotic cells (lower panel).

1.0 h, 26.5 mg/L/h, and 5.2 h, respectively. Compared to the intact IgG cetuximab ($C_{max} = 66$ mg/L, $T_{max} = 3$ h, $AUC = 3,182$ mg/L/h, $t_{1/2} = 37.8$), MI061 was pharmacokinetically

different because of its smaller size (Fig. 4). Typically, antibody fragments, including Fab' and F(ab')₂, have a lower PK values, higher penetration rate, and higher

kidney clearance rate than the whole IgG. According to PK parameters, inhibition of tumor growth by MI061 was monitored in HT29.

Tumor volume gradually increased throughout the 16-day period and reached a maximum of 380 mm³ in PBS-treated mice. However, in the cetuximab-injected mice and the MI061-treated xenograft (qd, i.p.), tumor growth was significantly suppressed and reached only 43 and 74% of the maximum tumor volume in PBS-treated mice, respectively, on day 16 (Fig. 4A). This was consistent with size measurements of the tumor masses excised from the xenografts (Fig. 4B); the tumor masses were much smaller than in PBS-treated mice. These results showed that, like cetuximab, MI061 could significantly inhibit tumor growth.

Apoptosis is one of the major mechanisms of cell death in response to anticancer agents, such as antibodies. Because cetuximab has been shown to induce apoptosis in various cell lines by several mechanisms [5,12,13], the induction of HT29 cell apoptosis by MI061 was investigated. The apoptotic effect of MI061 was analyzed by calculating the percentage of apoptotic cells using propidium iodide staining. In HT29 cells, the apoptotic effects of both cetuximab (24%) and MI061 (16%) were greater than in untreated control cells (5%) (Fig. 4), indicating that both have significant anti-cancer activity.

4. Discussion

The first attempt to produce recombinant antibodies in bacteria was hampered due to misfolding and aggregation in the bacterial cytoplasm [14,15]. Recently, however, minimized antibody fragments, including scFvs and Fabs, have been successfully expressed in a bacterial host through improved recombinant DNA technology and antibody engineering [16]. Antibody fragments have been used for various purposes ranging from simple investigational tools, such as diagnostic reagents, to highly refined biopharmaceutical drugs [3]. Recently, attempts were made to develop genetically engineered radiolabeled minibodies as potential PET imaging agents for specific targeting of cancers [17-19].

In this study, MI061 exhibiting significant anti-cancer activity against EGFR was successfully expressed in and purified from *E. coli*. Notably, while MI061 was highly expressed, it mostly accumulated in the cytoplasm and periplasm as misfolded aggregates. The PelB leader sequence gave the best minibody yield, which was probably attributed to a good combination of signal sequence and mature protein. According to Sletta *et al.* [20], leader sequence affects expression level of the gene by stabilizing the secondary structure of mRNA. Protein productivity by MI061/*E. coli* BL21(DE3) was highest in the YM9 glucose

medium, probably due to the large amount of yeast extract, a source of trace components, that can relieve cellular stress responses of *E. coli* [21]. Similarly, a high concentration of phosphate was known to be important for providing a buffering capacity and attaining high cell density of *E. coli*, by circumventing phosphate limitation [22].

Anti-tumor activity of purified MI061 in HT29 xenografted model was also significant but lower compared to cetuximab. We previously reported that anti-tumor effectiveness of MI061 was higher compared to cetuximab in A431 xenografted model [4]. Therefore, anti-tumor effectiveness of MI061 minibody seems to be influenced by the type of carcinoma cell lines.

Many proteins, including antibodies, contain disulfide bonds that must be correctly formed for a protein to be functional [23]. Since MI061 contains four cysteine residues that form two disulfide bonds in the scFv domain and two cysteine residues that form a disulfide bond in the C_{H3} domain, correct disulfide bond formation between cysteine residues is especially necessary for successful MI061 folding. The disulfide bond (Dsb) protein family facilitates folding by catalyzing the formation and isomerization of protein disulfide bonds in the periplasm. Thus, we plan to carry out further studies of the co-expression of MI061 and Dsb proteins to enhance protein folding in the periplasm.

Typically, antibody fragments, such as scFvs and Fabs, and engineered variants, such as single domain antibodies, diabodies, triabodies, and minibodies, have lower PK parameters (AUC and t_{1/2}) than intact IgG. In this study, MI061 indeed displayed significantly lower PK parameters than cetuximab. To overcome the disadvantages of lower PK, such as short serum half-life due to fast kidney clearance, some drug modification strategies, including PEGylation using chemical modification and PASylation using protein modification, may be applicable. PEGylation has emerged as an important technology for its biomedical properties, including prolonged circulating half-life, reduced toxicity, enhanced solubility and stability, and reduced proteolysis, and has been used in about 10 clinical protein and peptide drugs to date [24]. PASylation was recently described as an alternative technique that allows for the preparation of several types of therapeutic proteins and peptides with enhanced PK and *in vivo* activities [25]. Thus, we are currently attempting to generate a chemical conjugate with PEGylation and a genetic conjugate with PASylation on the cetuximab-based minibody.

On the other hand, minimizing the size and reducing the molecular weight of the minibody is expected to allow enhanced tumor penetration. Therefore, we are also further investigating the anti-cancer activity of MI061 by examining PK and biodistribution properties in an HT29 xenograft model.

In conclusion, as an anti-cancer therapeutic treatment, the genetically engineered minibody is a structurally and functionally adequate alternative inhibitor of EGFR signaling, and an *E. coli* expression system is an effective strategy for the production of anti-cancer antibodies.

Acknowledgement

This work was supported by a grant from the National Institute of Biological Resources (NIBR), funded by the Ministry of Environment (MOE) of the Republic of Korea (NIBR201529201).

Reference

1. Thomas, S. M. and J. R. Grandis (2004) Pharmacokinetic and pharmacodynamic properties of EGFR inhibitors under clinical investigation. *Cancer Treat Rev.* 30: 255-268.
2. Wu, X., M. Rubin, Z. Fan, T. DeBlasio, T. Soos, A. Koff, and J. Mendelsohn (1996) Involvement of p27KIP1 in G1 arrest mediated by an anti-epidermal growth factor receptor monoclonal antibody. *Oncogene.* 12: 1397-1403.
3. Holliger, P. and P. J. Hudson (2005) Engineering antibody fragments and the rise of single domains. *Nat. Biotech.* 23: 1126-1136.
4. Kim, Y. P., D. Park, J. J. Kim, W. J. Chi, S. H. Lee, S. Y. Lee, S. Kim, J. M. Chung, J. Jeon, B. D. Lee, J. H. Shin, Y. I. Lee, H. Cho, J. M. Lee, and H. C. Kang (2014) Effective therapeutic approach for head and neck cancer by an engineered minibody targeting the EGFR receptor. *PLoS one* 9: e113442.
5. Whitlow, M., B. A. Bell, S. L. Feng, D. Filpula, K. D. Hardman, S. L. Hubert, M. L. Rollence, J. F. Wood, M. E. Schott, D. E. Milenic, T. Yokota, and J. Schlom (1993) An improved linker for single-chain Fv with reduced aggregation and enhanced proteolytic stability. *Protein Eng.* 6: 989-995.
6. Keen, N. T. and S. Tamaki (1986) Structure of two pectate lyase genes from *Erwinia chrysanthemi* EC16 and their high-level expression in *Escherichia coli*. *J. Bacteriol.* 168: 595-606.
7. Movva, N., K. Nakamura, and M. Inouye (1980) Amino acid sequence of the signal peptide of ompA protein, a major outer membrane protein of *Escherichia coli*. *J. Biol. Chem.* 255: 27-29.
8. Humpreys, D. P., M. Sehdev, A. P. Champman, R. Ganesh, B. J. Smith, L. M. King, D. J. Glover, D. G. Reeks, and P. E. Stephens (2000) High-level periplasmic expression in *Escherichia coli* using a eukaryotic signal peptide: Importance of codon usage at the 5' end of the coding sequence. *Protein Expr. Purif.* 20: 252-264.
9. Schmiedl, A., F. Breitling, and S. Dubel (2000) Expression of a bispecific dsFv-dsFv' antibody fragment in *Escherichia coli*. *Protein Eng.* 13: 725-734.
10. Matsuo, T., S. S. Nishizuka, K. Shida, T. Iwaya, M. Ikeda, and G. Wakabayashi (2011) Analysis of the anti-tumor effect of cetuximab using protein kinetics and mouse xenograft models. *BMC Res. Notes* 4: 140.
11. Lee, Y. J., S. J. Chung, and C. K. Shim (2007) BA Calc 2007® for Windows®, Version 1.0.0.
12. Li, X. and Z. Fan (2010) The epidermal growth factor receptor antibody cetuximab induces autophagy in cancer cells by down-regulation HIF-1 alpha and Bcl-2 and activation the beclin 1/hVps34 complex. *Cancer Res.* 70: 5942-5952.
13. Li, X. Y. Lu, K. Liang, T. Pan, J. Mendelsohn, and Z. Fan (2008) Requirement of hypoxia-inducible factor-1alpha down-regulation in mediating the antitumor activity of the anti-epidermal growth factor receptor monoclonal antibody cetuximab. *Mol. Cancer Ther.* 7: 1207-1217.
14. Boss, M. A., J. H. Kenten, C. R. Wood, and J. S. Emtage (1984) Assembly of functional antibodies from immunoglobulin heavy and light chains synthesized in *Escherichia coli*. *Nucleic Acids Res.* 12: 3791-3806.
15. Cabilly, S., A. D. Riggs, and H. Pande (1984) Generation of antibody activity from immunoglobulin polypeptide chains produced in *Escherichia coli*. *Proc. Natl. Acad. Sci.* 81: 3273-3277.
16. Ahmad, Z. A., S. K. Yeap, A. M. Ali, W. Y. Ho, N. B. Alitheen, and M. Hamid (2012) scFv antibody: Principles and clinical application. *Clin. Dev. Immunol.* Doi:10.1155/2012/980250.
17. Kenanova, V., T. Olafsen, D. M. Crow, G. Sundaresan, M. Subbarayan, N. H. Carter, D. N. Ikle, P. J. Yazaki, A. F. Chatziaoanou, S. S. Gambhir, L. E. Williams, J. E. Shively, D. Colcher, A. A. Raubitschek, and A. M. Wu (2005) Tailoring the pharmacokinetics and positron emission tomography imaging properties of anti-carcinoembryonic antigen single-chain Fv-Fc antibody fragments. *Cancer Res.* 65: 622-631.
18. Pettersen, E. F., T. D. Goddard, C. C. Huang, G. S. Couch, D. M. Greenblatt, E. C. Meng, and T. E. Ferrin (2004) UCFS Chimera-A visualization system for exploratory research and analysis. *J. Comput. Chem.* 25: 1605-1612.
19. Wong, J. Y., D. Z. Chu, L. E. Williams, D. M. Yamauchi, D. N. Ikle, C. S. Kwok, A. Liu, S. Wilczynski, D. Colcher, P. J. Yazaki, J. E. Shively, A. M. Wu, and A. A. Raubitschek (2004) Pilot trial evaluating an ¹²⁵I-labeled 80-kilodalton engineered anticarcinoembryonic antigen antibody fragment (cT84.66 minibody) in patients with colorectal cancer. *Clin. Cancer Res.* 10: 5014-5021.
20. Sletta, H., A. Tondervick, S. Hakvag, T. E. Vee Anune, A. Nedel, R. Aune, G. Evensen, S. Valla, T. E. Ellingsen, and T. Brautaset (2007) The presence of N-terminal secretion signal sequences leads to strong stimulation of the total expression levels of three tested medically important proteins during high-cell-density cultivations of *Escherichia coli*. *Appl. Environ. Microbiol.* 73: 906-912.
21. Lim, H. K., K. H. Jung, D. H. Park, and S. I. Chung (2000) Production characteristics of interferon-alpha using an L-arabinose promoter system in a high-cell-density culture. *Appl. Microbiol. Biotechnol.* 53: 201-208.
22. Korz, D. J., U. Rinas, K. Hellmuth, E. A. Sanders, and W. D. Deckwer (1995) Simple fed-batch technique for high cell density cultivation of *Escherichia coli*. *J. Biotechnol.* 39: 59-65.
23. Choi, J. H. and S. Y. Lee (2004) Secretory and extracellular production of recombinant proteins using *Escherichia coli*. *Appl. Microbiol. Biotechnol.* 64: 625-635.
24. Jevsevar, S., M. Kunstelj, and V. G. Porekar (2010) PEGylation of therapeutic proteins. *Biotechnol. J.* 5: 113-128.
25. Schlapschy, M., U. Binder, C. Börger, I. Theobald, K. Wachinger, S. Kisling, D. Haller, and A. Skerra (2013) PASylation: A biological alternative to PEGylation for extending the plasma half-life of pharmaceutically active proteins. *Protein Eng. Des. Sel.* 26: 489-501.